



Oriented Functionalization of Natural Hollow Kapok Fiber for Highly Efficient Removal of Toxic Hg(II) from Aqueous Solution

Feng Wang^{1,2}, Yian Zheng^{1,3*}, Yongfeng Zhu^{1,2} and Aiqin Wang^{1*}

¹ Center of Eco-material and Green Chemistry, Lanzhou Institute of Chemical Physics, Chinese Academy of Science, Lanzhou, China, ² University of the Chinese Academy of Sciences, Beijing, China, ³ Gansu Key Laboratory for Environmental Pollution Prediction and Control, College of Earth and Environmental Sciences, Lanzhou University, Lanzhou, China

OPEN ACCESS

Edited by:

Leonardo Fernandes Fraceto,
São Paulo State University - Unesp,
Brazil

Reviewed by:

Daiana Avila,
Universidade Federal do Pampa,
Brazil
Renato Grillo,
International Iberian Nanotechnology
Laboratory, Portugal

*Correspondence:

Yian Zheng
zhengya@lzu.edu.cn;
Aiqin Wang
aqwang@licp.cas.cn

Specialty section:

This article was submitted to
Green and Environmental Chemistry,
a section of the journal
Frontiers in Environmental Science

Received: 12 November 2015

Accepted: 13 January 2016

Published: 04 February 2016

Citation:

Wang F, Zheng Y, Zhu Y and Wang A
(2016) Oriented Functionalization of
Natural Hollow Kapok Fiber for Highly
Efficient Removal of Toxic Hg(II) from
Aqueous Solution.
Front. Environ. Sci. 4:4.
doi: 10.3389/fenvs.2016.00004

Due to hollow and tubular structure, a natural kapok fiber (KF) was used as the support and orientation matrix to control the polymerization of ethyleneglycol dimethacrylate (EGDMA) and *N*-vinylimidazole (VIM) along its inherent axial surface via a facile *in situ* rapid polymerization reaction in air atmosphere. The as-formed KF@VIM/EGDMA composite is featured with porous surface and rich *N*-containing functional groups for potential application as a highly efficient adsorbent for removal of toxic Hg(II) from aqueous solution. The variables affecting the adsorption capacity were studied, including monomer ratio, external pH values, contact time, and initial Hg(II) concentration. The pseudo-second-order equation and two adsorption isotherms including Langmuir and Freundlich equations were applied to determine the adsorption kinetics and adsorption capacity. The results show that the as-prepared KF@VIM/EGDMA composite has a maximum adsorption capacity of 697 mg/g to Hg(II), while no appreciable adsorption capacity can be found for KF itself. Given its intrinsic large lumen, faster adsorption kinetics (45 min) are also expected and observed for KF@VIM/EGDMA. After a simple filtration, this adsorbent can be directly separated from the aqueous solution and then be regenerated for multi-cyclable utilization. During the adsorption process, the chemical complexing represents the main adsorption mechanism. As a naturally renewable KF, such a simple preparation method opens a new avenue to develop highly efficient and economically viable adsorbent for removal of toxic heavy metal from aqueous solution.

Keywords: kapok fiber, oriented, *N*-vinylimidazole, selective adsorption, Hg(II)

INTRODUCTION

Owing to high surface-to-mass ratio, bio-compatibility, good mechanical performance and ability to be shaped in various forms, many natural or man-made microfibers have been directly utilized or modified as an ideal substrate material for loading active nanoparticles (El Ghali et al., 2012; Xia et al., 2013). Among them, kapok fiber (KF) is obtained from the fruits of the kapok tree (Zheng et al., 2012), and is a kind of single-cell natural cellulose fiber with about 64% cellulose, 13% lignin, 2.5% xylan, and 0.8% wax (Liu et al., 2012b). KF is the lightest, thinnest, and highest hollow degree material among the natural ecological fibers and exhibits fluffy, low density, non-allergic, non-toxic, better surface activity, good oil absorptivity, resistant to rot, and water-repellent nature

(Lim and Huang, 2007; Liu et al., 2012b). Therefore, KF has been traditionally used as the stuffing for bedding, life preservers, upholstery, and water-safety equipment and for insulation against sound and heat (Liu et al., 2012b). Structured with rather fine natural microtubules (ca. 8–10 μm in diameter and ca. 0.8–1.0 μm in wall thickness) (Chung et al., 2008) with the hollow rate of above 86% (Kang et al., 2007), this fiber shows also its potential for various new application fields, especially as the support for active nanoparticles and as the biotemplate to prepare a series of microtubes originated from organic or inorganic materials (Zheng et al., 2014). KF is an insoluble natural polymer with a hollow and large lumen, and then it is anticipated to guide the growth orientation of a polymerizable monomer to avoid the agglomeration of polymer and enlarge the specific surface. Accordingly, the resulting KF composites can be easily separated or recovered from liquid system (Huang and Lim, 2006; Abdullah et al., 2010). Furthermore, the orientated growth of a polymerizable monomer on the surface of KF can afford the resulting material with tailored functional groups for promising application as an excellent adsorbent for removal of a targeted pollutant.

Mercury (Hg) is one of the most hazardous heavy metals included on the US Environmental Protection Agency's (EPA) list of priority pollutants (Idris et al., 2011). Due to its persistence and bio-accumulation in the food chain (Shan et al., 2015), this metal is extremely harmful to both public health and aquatic life and thus, the removal of Hg(II) from aqueous solutions has attracted increasing attention. Adsorption is an important and useful technology for removal of heavy metal ions from aqueous solution and the core of this technology is to develop a novel kind of adsorbent. Up to date, this technology shows little/no selectivity in generally (Idris et al., 2011) and the large capital and high regeneration costs of adsorbent should also be stressed for wastewater treatment (Uğuzdoğan et al., 2009). Therefore, functional modification of abundant natural polymers in particular for those plant materials with metal chelating sites seems to be a useful method to overcome these problems (Zheng et al., 2014). One can speculate that KF may be a promising alternative for developing such a novel adsorbent with tailored functionality by modifying it by a polymer coating with high affinity to Hg(II).

As a kind of nitrogen-substituted aromatic heterocycle, *N*-vinylimidazole (VIM) is considered to be one of the most favorable species with great chelating tendency for Hg(II) (Kara et al., 2005; Bessbousse et al., 2010). Sun et al. (2013) prepared a silica-based adsorbent by γ -radiation induced grafting of VIM on the silica arisen from chlorotrimethylsilane, and the adsorption capacity of the as-prepared adsorbent for Hg(II) was as high as 355.9 mg/g in $\text{HgCl}_2/\text{HNO}_3$ solution at pH 5. Shan et al. (2015) modified the $\text{Fe}_3\text{O}_4/\text{SiO}_2$ magnetic nanoparticles by grafting poly(*N*-vinylimidazole) oligomer to fabricate an adsorbent (FSPV) to remove Hg(II) from water and found that the Hg(II) adsorption capacity of FSPV was 346 mg/g at pH 7 and 25°C in 10 mM NaCl. Thus, orientated growth of polymerizable VIM along the KF surface will be a feasible plan for developing an adsorbent with high affinity for Hg(II). Furthermore, the insolubility of KF enables the as-formed composite to be

easily separated or recovered from liquid system. However, the existence of waxy coating on KF makes it hydrophobic, and accordingly, this fiber is gaining much attention as an alternative for oil removal (Ali et al., 2011; Wang et al., 2013a), but rarely in aqueous solution (Duan et al., 2013). Therefore, it is a prerequisite to change the wettability of KF from original hydrophobicity to hydrophilicity so as to remove pollutants from aqueous solution efficiently. It is reported that when KF was treated with sodium chlorite (NaClO_2) under acidic condition, the surface wax can be efficiently removed while its hollow lumen can be perfectly retained (Keshk et al., 2006; Kang et al., 2007).

Based on above background, KF used in this study can be firstly pre-treated with NaClO_2 under acidic condition, and the treated KF can then be coated with VIM as the metal chelating sites, using ethyleneglycol dimethacrylate (EGDMA) as both of comonomer and crosslinker by a facile step to achieve a cheap adsorbent KF@VIM/EGDMA with efficient selectivity and high regeneration for Hg(II) removal. The specific objectives of this study are (i) optimization of the ratio of EGDMA to VIM and the amount of KF for preparation of the adsorbent; (ii) preparation of a fiber-like KF@VIM/EGDMA with unique morphology and easy separation or recovery ability from liquid system; and (iii) evaluation of the efficacy of the as-prepared KF@VIM/EGDMA composite for Hg(II) removal.

EXPERIMENTAL METHODS

Materials

KF was purchased from Shanghai Panda Co. Ltd., China. *N*-vinylimidazole (VIM, 99%) was purchased from Alfa Aesar Chemical Co., Ltd., Tianjin, China. Ethylene glycol dimethacrylate (EGDMA, >97%) was provided by Tokyo Chemical Industry Co., Ltd. 2,2'-azobis(2-methylpropionitrile) (AIBN, AR) was received from Tianjin Kaixin Chemical Industry Co., Ltd., China. Hydrochloric acid (HCl), sodium hydroxide (NaOH) and other reagents used were all analytical-reagent grade. Deionized water was used throughout the experiments. All of above reagents were used without further purification.

Kapok Fiber Treated by NaClO_2

Kapok fiber (1.5 g) was pre-treated with 100 mL of the mixture solution of NaClO_2 (0.93 g) and glacial acetic acid (1.42 mL) at 90°C for 1 h. The treated KF was washed with distilled water until the filtrate reached pH 6–7, then dried at 70°C to a constant weight. The treated KF was whiter than the pristine one as a result of bleaching property of NaClO_2 .

Preparation of Poly(*N*-vinylimidazole-Co-Ethylene Glycol Dimethacrylate)

For the preparation of poly(*N*-vinylimidazole-co-ethylene glycol dimethacrylate) (P(VIM-co-EGDMA)) with high affinity to Hg(II), the monomer ratio of EGDMA to VIM was firstly optimized according to the following procedure (Table S1): a designed amount of EGDMA and VIM (2 g) were dissolved into 10 ml methanol using 0.08 g AIBN as the initiator for free-radical

polymerization. After the reactions were proceeded in an oven at 60°C for 24 h to obtain some white powder, the resulting products were washed with distilled water and centrifugated for several times, and then dried at 40°C in an oven to a constant weight.

Preparation of KF@VIM/EGDMA Composites

According to the optimization condition of Section Preparation of Poly(N-vinylimidazole-Co-Ethylene Glycol Dimethacrylate), a series of KF-based composite adsorbents were prepared by the following procedure: A predetermined amount of KF (Table 1) was added into 5 mL of methanol containing 0.75 g EGDMA, 1.0 g VIM and 0.04 g AIBN, then the reaction was performed in an oven under 60°C for 24 h to obtain the products. After the reaction was finished, the resulting adsorbents were washed with distilled water for several times, filtered with a normal sieve and dried at 40°C in an oven to a constant weight. Scheme 1 showed the schematic diagram of the structure and formation of KF@VIM/EGDMA.

Characterizations

The surface morphology was observed using a field emission scanning electron microscope (FESEM, JSM-6701F, JEOL) after coating the samples with gold film. FTIR spectra of samples were recorded on a Thermo Nicolet NEXUS spectrometer in 4000–400 cm⁻¹ wavenumber region using KBr pellets, with a KBr:sample ratio of 100:1. XRD patterns were collected on a X'pert PRO X-ray power diffractometer (PAN analytical Co., Netherlands) using Cu-K_α radiation of 1.5406 Å (40 kV, 30 mA). X-ray photoelectron spectroscopy (XPS) was recorded on a PHI 5702 spectrometer equipped with a monochromatic Al K_α X-ray source. Thermogravimetry (TG) analysis of the samples was recorded by a Diamond TG-DTA 6300 thermoanalyzer instrument from 30 to 800°C at a heating rate of 10°C min⁻¹ under a nitrogen atmosphere.

The point of zero charge (pH_{PZC}) was measured by an immersion technology according to the following process (Bourikas et al., 2003): adjusting the series aqueous solutions with varying pH values by adding 0.1 and 1.0 mol/L HCl or NaOH solutions, and then suspending 50 mg adsorbent sample in the solutions. The aqueous suspensions were equilibrated for 24 h to reach an equilibrium pH value, and then the pH value of each suspension was measured with a digital pH meter (Mettler-Toledo, FE20). The ΔpH was then determined from the pH change between the solution without and with the adsorbent, i.e., ΔpH = pH(blank solution) – pH(suspension). The pH_{PZC} was identified as the pH where the minimum ΔpH-value was obtained. The zeta potentials were obtained by injecting the

suspension into the electrophoresis cell and measuring them with a Malvern Zetasizer Nano-ZS apparatus.

Adsorption Experiments

The batch adsorption experiments were carried out to evaluate the adsorption capacity of KF@VIM/EGDMA. Adsorption experiments were carried out by dispersing 20 mg of adsorbent into 25 mL of heavy metal solutions in a thermostatic shaker (THZ-98A, Chincan, Zhejiang, China) at 30°C and 130 rpm for a given time to achieve the adsorption equilibrium. After filtration, all the supernatant was left for further analysis to obtain the corresponding adsorption capacity. The concentrations of heavy metal ions in the solution were measured by ultraviolet spectrophotometry with a Specord 200UV/vis spectrophotometer at the maximum absorbency wavelength (456 nm for Cu²⁺, 550 nm for Pb²⁺, 582 nm for Cd²⁺, 548 nm for Zn²⁺, and 558 nm for Hg(II) using 2,9-dimethyl-1,10-phenanthroline (for Cu²⁺), xylenol orange (for Pb²⁺ and Cd²⁺), 1-(2-pyridylazo)-2-naphthol (for Zn²⁺) and safranin T (for Hg(II)) as the respective complexing agents. The amount of heavy metal ions adsorbed (*q*, mg/g) was calculated according to the following formulas:

$$q = \frac{(C_0 - C_e) \times 0.025}{m} \quad (1)$$

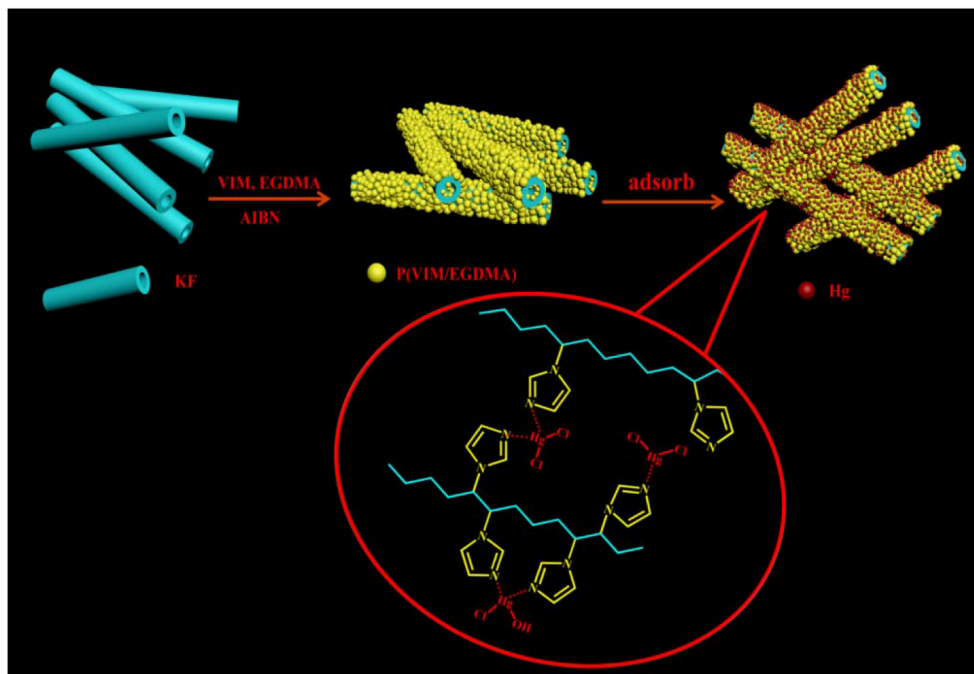
Here, *q* is the amount of metal ion adsorbed at equilibrium (mg/g), *C*₀ (mg/L) is the initial concentration, *C*_{*e*} (mg/L) is the equilibrium concentration (mg/L), 0.025 is the volume of the adsorbate solution (L), and *m* is the mass of the adsorbent used (g). All of these experiments were carried out in triplicate to assure the results were reproducible, and the relative standard deviation was less than 5% in this study.

The HgCl₂ solution with initial concentration of 300 mg/L was used to evaluate the adsorption capacity of the series P(VIM-co-EGDMA) and KF@VIM/EGDMA adsorbents to optimize the monomer ratio of EGDMA to VIM and the amount of KF. For the KF@VIM/EGDMA composite, selective adsorption was performed under non-competitive conditions by using single CuCl₂, PbCl₂, ZnCl₂, CdCl₂, HgCl₂ solution with each concentration of 300 mg/L as the model. The required pH of solution was adjusted by 0.1 mol/L NaOH and HCl solutions. Batch adsorption experiments were carried out with a freshly prepared HgCl₂ solution with an initial concentration of 400 mg/L at different contact time to study the adsorption kinetic. The adsorption capacity of Hg(II) onto KF@VIM/EGDMA was determined using an increasing concentration from 100 to 1000 mg/L.

In order to evaluate the reusability, the influences of different desorbing agent and desorbing agent concentration on desorption efficiency were firstly studied to figure out the optimum desorption conditions. Firstly, 0.5 mol/L H₂SO₄, thiourea, HCl and KI solution were used as the desorption media. Then the effects of initial concentration of a chosen desorption medium on the desorption efficiency were evaluated. After that, the following procedures were performed to study the reusability of the as-prepared adsorbent: 20 mg adsorbent was mixed with

TABLE 1 | Formulation for KF@VIM/EGDMA dispersion.

| Serial number | 1 | 2 | 3 | 4 | 5 |
|---------------|---|-----|-----|-----|-----|
| KF (g) | 0 | 0.3 | 0.4 | 0.5 | 0.6 |



SCHEME 1 | The representation of a possible structure of KF@VIM/EGDMA and its adsorption for Hg(II).

25 mL HgCl_2 solution (300 mg/L) for 2 h. After the adsorption equilibrium, the KF@VIM/EGDMA was desorbed with 25 mL chosen desorbing agent solution for 5 h. Before the next cycle, the adsorbent was filtered and washed with distilled water for several times, and was neutralized with NaOH solution for 10 min, then washed with distilled water till the pH reached about 5.5. The consecutive adsorption-desorption process was performed for seven times to test the reusability of the composite.

Isotherm and Kinetics Models

The models of Langmuir (Equation 2) and Freundlich (Equation 3) were used to fit the isotherm equations to the experimental data and calculate the theoretical maximum adsorption capacity (Alila and Boufi, 2009).

$$\text{Langmuir equation: } \frac{C_e}{q_e} = \frac{1}{q_m b} + \frac{C_e}{q_m} \quad (2)$$

$$\text{Freundlich equation: } \log q_e = \log K + (1/n) \log C_e \quad (3)$$

Here C_e (mg/L) is the equilibrium concentration of Hg(II), q_e (mg/g) is the equilibrium adsorption capacity, and q_m (mg/g) is the theoretical maximum value of adsorption capacity, b (L/g) is the Langmuir adsorption constant representing the free energy of adsorption. n (dimensionless) and K (L/g) are the heterogeneity factor and the Freundlich isotherm constant, respectively. $1/n$ indicates the bond distribution and K represents the strength of the adsorptive bond related to the adsorption capacity.

Among various established kinetic models, the pseudo-first-order (Equation 4) and pseudo-second-order (Equation 5)

kinetic models are considered as the most commonly used models to investigate the mechanism ruling the adsorption process and quantify the changes in adsorption with time (Oo et al., 2009).

$$\text{Pseudo-first-order: } \log (q_e - q_t) = \log q_e - \left(\frac{k_1}{2.303} \right) t \quad (4)$$

$$\text{Pseudo-second-order: } \frac{t}{q_t} = \frac{1}{(k_2 \times q_e^2)} + \frac{t}{q_e} \quad (5)$$

Here q_t and q_e are the adsorption capacities of the adsorbent at time t (s) and at equilibrium, respectively. k_1 (min^{-1}) and k_2 (g/mg min) are the rate constants of the pseudo-first-order equation and pseudo-second-order equation, respectively. Kinetic constants k and q_e were calculated from the slopes and intercepts of the plots of $\log (q_e - q_t)$ vs. t and t/q_t vs. t , respectively.

RESULTS AND DISCUSSION

Formation of KF@VIM/EGDMA

During the formation of KF@VIM/EGDMA, the involved reaction mechanism is a typical free radical polymerization. When the temperature reached 60°C , the initiator AIBN was decomposed to produce a radical which can initiate the polymerization. At the same time, the P(VIM-co-EGDMA) particles were formed in the dispersion and deposited on the fiber surface (Fan et al., 2012). With the proceeding of polymerization reaction, the surface of KF was coated by a thin layer of polymer coating consisted of P(VIM-co-EGDMA), as shown in **Scheme 1**.

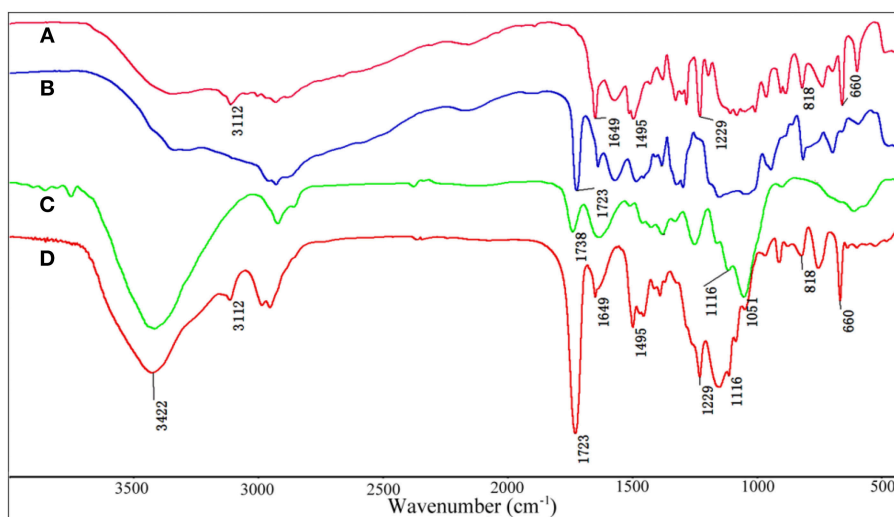


FIGURE 1 | FTIR spectra of (A) VIM, (B) EGDMA, (C) KF and (D) KF@VIM/EGDMA.

The point of zero charge (pH_{PZC}) and isoelectric point (pH_{IEP}) were measured by immersion technique and zeta potential measurements to understand the formation of adsorbent better. As shown in Figure S1, the pH_{PZC} is 7.7 for KF@VIM/EGDMA and 7.2 for P(VIM-co-EGDMA), while the pH_{IEP} is 7.8 for KF@VIM/EGDMA and 8.4 for P(VIM-co-EGDMA). The difference between pH_{PZC} and pH_{IEP} would give an indication of the surface charge distribution of the adsorbents. Compared the pH_{IEP} with pH_{PZC} , the equal value of them would indicate the similar positively charged external surface and the interior of KF@VIM/EGDMA, suggesting that the inner wall of KF was also coated with polymer layer. In addition, the pH_{PZC} and pH_{IEP} values for KF@VIM/EGDMA are closer than that of P(VIM-co-EGDMA), suggesting a more homogeneous surface of KF@VIM/EGDMA (Strelko Jr et al., 2002).

FTIR Analysis

The FTIR spectra of VIM (Figure 1A), EGDMA (Figure 1B), KF (Figure 1C), and KF@VIM/EGDMA (Figure 1D) are shown in Figure 1. The FTIR spectrum of KF@VIM/EGDMA (Figure 1D) is similar to that of KF (Figure 1C) except several characteristic absorption bands originated from VIM (Figure 1A) and EGDMA (Figure 1B). The broad band of KF at about 3422 cm^{-1} derived from the stretching vibration of O-H in cellulose had almost no change after modification. The ester bands of KF at 1738 cm^{-1} which was ascribed to the vibration of C=O was merged with the other carbonyl bond at 1723 cm^{-1} of EGDMA to create a strong and sharp absorption band in KF@VIM/EGDMA spectrum at 1723 cm^{-1} . The absorption bands at 3112 cm^{-1} in the spectrum of KF@VIM/EGDMA was assigned as the stretching vibration of the =CH in the ring of VIM (Sun et al., 2013), and the narrow peak at 1229 cm^{-1} was ascribed to chain C-H bending with C=N stretching of imidazole (Talu et al., 2015). The band observed at 1495 cm^{-1} (Figures 1A,D) was assigned to the C-H bending vibrations of the aliphatic

chain in coupling with the C-C and C=N ring stretching vibrations of VIM (Sun et al., 2013). Furthermore, the narrow band at 1649 cm^{-1} in VIM spectrum which attributed to the characteristic of C=C stretching vibration and the characteristic band of puckering vibration of imidazole ring at 660 cm^{-1} were also appeared in the KF@VIM/EGDMA spectrum. The characteristic absorption bands of VIM and EGDMA appeared in the FTIR spectrum of KF@VIM/EGDMA confirm that KF is combined successfully with polymers.

SEM Morphology

The photographs of the raw and modified KF presented in Figures 2A,B show that the raw KF is coated with polymer successfully and the as-prepared adsorbent has a fibrous shape. The FE-SEM images show that the raw KF presents regular hollow tubular structure with a smooth surface (Figure 2C). After being modified, both of external surface and inner wall are all covered with plenty of highly aggregated polymer particles with rough surface (Figures 2D-F). Therefore, it can be concluded that KF can provide a wonderful substrate material to orient the growth of polymerizable monomers to form the KF@VIM/EGDMA fiber with amazing microstructure.

XRD Analysis

The crystalline structures of the native and the modified KF were also investigated by means of XRD technology. As can be seen from Figure 3A, the characteristic diffraction peaks of KF appear at 2θ of 15.78° , 22.62° , and 34.96° , which correspond to the (110), (200) and (004) crystallographic planes, respectively (Liu et al., 2012a). Otherwise, the XRD pattern of KF@VIM/EGDMA (Figure 3B) shows significant changes in the crystalline peaks. The diffraction peak of KF at 2θ of 34.96° (004) has disappeared and the intensity of diffraction peak at 2θ of 22.62° (200) gets weaker, indicating that the aggregating crystalline phase has been

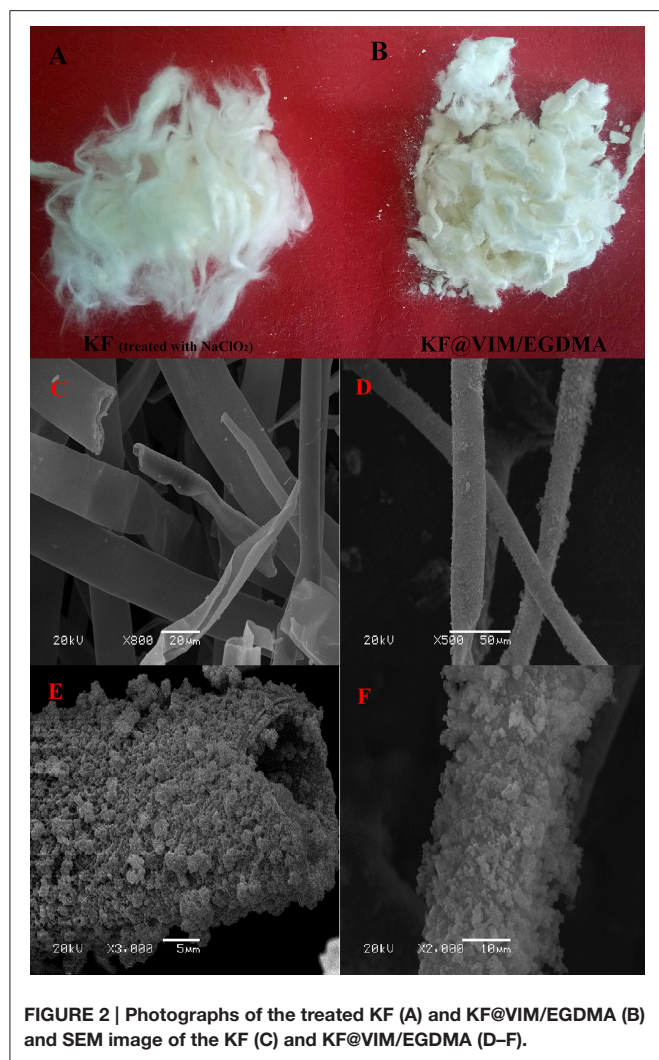


FIGURE 2 | Photographs of the treated KF (A) and KF@VIM/EGDMA (B) and SEM image of the KF (C) and KF@VIM/EGDMA (D–F).

greatly altered after modification. The XRD data indicate that KF is favorable to the attachment of polymer.

TG Analysis

Thermal analysis was performed to analyze the decomposition temperature and thermal stability of materials. The thermograms of the raw KF and KF@VIM/EGDMA are presented in **Figure 4**. The thermograms of KF and its composites showed the first weight loss at around 30–250°C. This was due to the evaporation of water (Prachayawarakorn et al., 2013). The sudden steep weight losses of KF (**Figure 4A**) started at 242°C and ended around 364°C with almost 70% weight loss. Then a slow degradation started below 364°C and ended at 619°C with a little weight loss of 19%. For the KF@VIM/EGDMA (**Figure 4B**), the thermogravimetry curve resembles apparently to that of KF. The maximum weight loss was occurred approximately at 269°C and ended near 411°C with an accompanying 51% weight loss. Then the followed degradation started from about 411 to 770°C. The results of thermal analysis suggested that the thermal stability of the KF@VIM/EGDMA composite was improved.

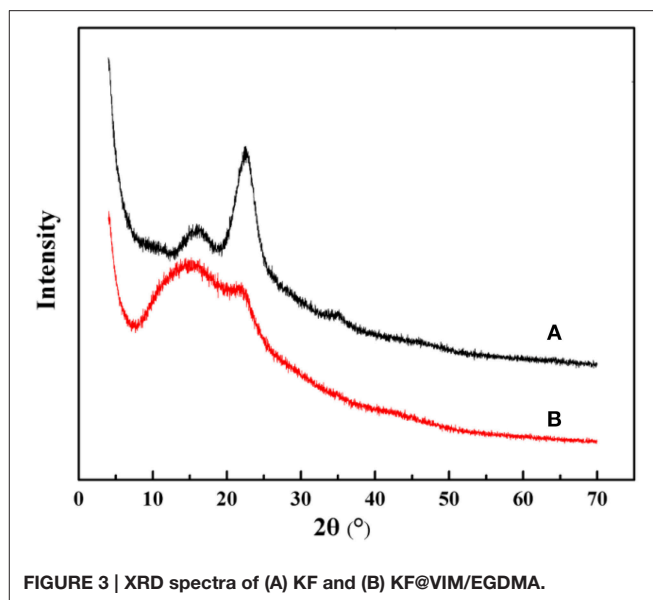


FIGURE 3 | XRD spectra of (A) KF and (B) KF@VIM/EGDMA.

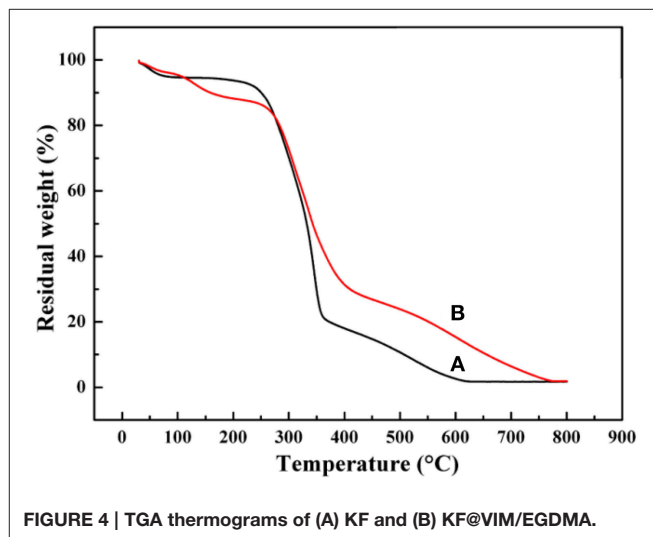


FIGURE 4 | TGA thermograms of (A) KF and (B) KF@VIM/EGDMA.

Effect of Monomer Ratio on Adsorption Capacity

The effects of EGDMA to VIM ratio on the adsorption capacity were investigated in **Figure 5**. It is clear that the adsorption capacities increased from 248.52 to 342.02 mg/g as the ratio of EGDMA to VIM was ranged from 3/2 (VIM%: 40.0%) to 1.5/2 (VIM%: 57.1%), beyond which the adsorption capacities showed a monotonic decrease. In general, increasing the VIM content is beneficial for the adsorption capacities, while excess VIM will result in a reduction in the adsorption capacity. The falling adsorption capacities of the adsorbent can be attributed to increasing steric hindrance of the imidazole ring as the VIM content increased. The large amount of VIM would impede the grafting of VIM, and accordingly, the adsorption capacity will be affected. This fact can be further testified by the decreasing yield. According to the results presented in **Figure 5**, the sample

with EGDMA/VIM ratio of 1.5/2 was adopted for further investigation.

Optimization of the Content of KF

There is no doubt that the content of KF will influence the adsorption properties significantly. As shown in **Figure 6A**, KF shows no appreciable adsorption for Hg(II). Therefore, it is not surprising that with increasing amount of KF, KF@VIM/EGDMA exhibits a decreasing adsorption capacity for Hg(II) (Zheng et al., 2012). Otherwise, too much KF will result in insufficiency use of KF and cause unnecessary waste, while too little amount of KF is insufficient to orientate the growth of polymers onto its surface. Thus, 0.3 g KF was finally selected for further studies.

Selective Adsorption of Hg(II)

The selective adsorption results of KF@VIM/EGDMA are summarized in **Figure 6B**. It was found that the adsorption

capacity for Hg(II) (286.20 mg/g) was much higher than the other four heavy metals [Cu(II) (32.12 mg/g), Pb(II) (20.08 mg/g), Cd(II) (17.47 mg/g) and Zn(II) (22.67 mg/g)], indicating that the as-prepared adsorbent exhibited obvious adsorption selectivity to Hg(II) due to different metal ion species between Hg(II) and the others in the aqueous solutions. Compared with ionic heavy metals, the major species of Hg(II) in the solution was present in the form of electroneutral species such as HgCl_2 and HgClOH that could promote the combination between Hg(II) and protonated imidazole ring to form the mercury-imidazole complex (Sun et al., 2013). The positive zeta potential values of KF@VIM/EGDMA at $\text{pH} < 7$ in aqueous solution (Figure S1) could explain the selectivity of the adsorbent for Hg(II) very well. Furthermore, the interaction between Hg(II) and imidazole ring did not break the Hg-Cl bond in HgCl_2 and HgClOH . All the information implies that the Hg(II) could be absorbed by KF@VIM/EGDMA via non-electrostatic forces (Shan et al., 2015).

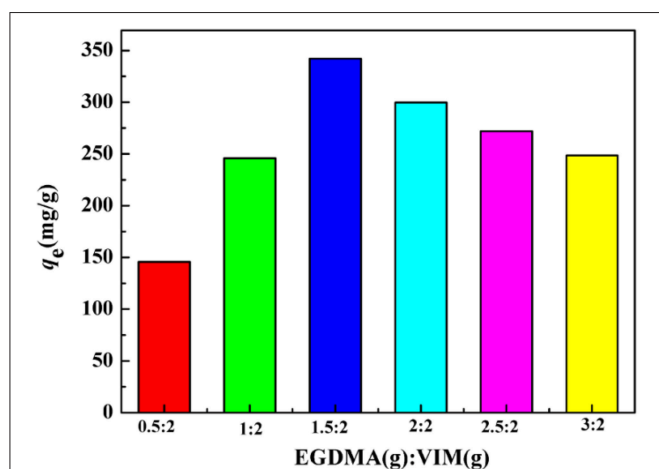


FIGURE 5 | The effect of EGDMA/VIM ratio on adsorption capacity.

Adsorption experiments: C_0 : 300 mg/L; sample dose: 20 mg/25 mL; pH: 5.5; temperature: 30°C; equilibrium time: 120 min.

Effect of pH

In general, the pH value has been considered as a significant parameter governing the extent of metal ion adsorption by an adsorbent as it influences both the surface properties of the adsorbent molecule (Shen et al., 2013; Kyzas et al., 2014), metal species and the availability of binding site of the adsorbate which depends on the functional group of an adsorbent (Afkhani et al., 2010). Since the metal species are mainly in the forms of precipitation at higher pH (Kampalananwat and Supaphol, 2014), so the adsorption experiments were carried out at the initial pH range from 1 to 6 with initial concentration of 200 and 500 mg/L to avoid the precipitation.

As the results shown in **Figure 7**, the adsorption capacities remarkably increase with increasing initial pH at the highly acidic condition ($\text{pH} < 4.0$) and obtained the maximum metal uptakes at close to neutral condition ($\text{pH} = 4-6$). The adsorption capacities could largely be affected by the competitive interaction between metal and hydrogen ions with the active sites on

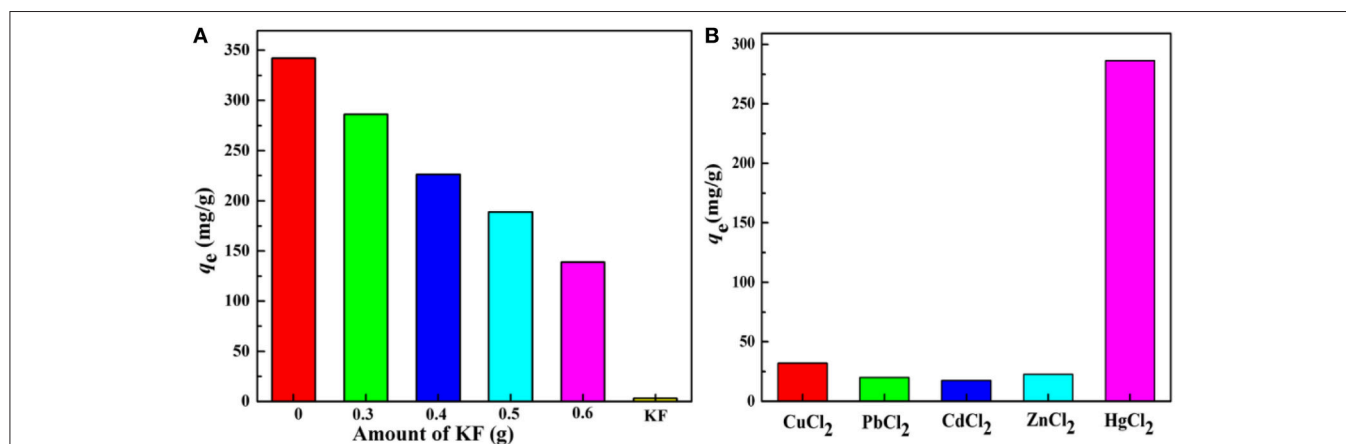


FIGURE 6 | (A) The effect of the amount of KF on adsorption capacity and (B) Adsorption capacities of KF@VIM/EGDMA adsorbents for various divalent heavy metal ions. Adsorption experiments: C_0 : 300 mg/L; sample dose: 20 mg/25 mL; pH: 5.5; temperature: 30°C; equilibrium time: 120 min.

the surface of the adsorbent at acidic conditions (Chen et al., 2008). The decreasing concentration of H^+ which resulted from the pH increased from 1 to 4 promoted the formation of the mercury-imidazole complex and increased the adsorption capacity of KF@VIM/EGDMA for Hg(II) (Sun et al., 2013). The protonation of imidazole groups in acidic conditions sharply increased the equilibrium pH of the heavy metal solutions (as shown in inset in Figure 7) and hindered the interaction between heavy metal cations and the adsorbent (Ijagbemi et al., 2010), resulting thus in the reducing number of binding sites available for metal ions uptake. The equilibrium adsorption capacities for Hg(II) were 262.76 and 653.34 mg/g when the initial concentration were fixed at 200 and 500 mg/L at pH 6.0, respectively. According to the results, a series of freshly prepared $HgCl_2$ solutions were directly used without adjusting their

pH-values since the original pH values for each concentration were all closed to 5.5.

Adsorption Isotherms

As the initial concentration of heavy metal ions has a significant influence on the adsorption capacity of the heavy metal ions, the equilibrium isotherms for the adsorption of Hg(II) by KF@VIM/EGDMA at 30°C were studied covering a wide range of initial concentrations, as shown in Figure 8A.

The isotherm results reveal the good adsorption capacity of KF@VIM/EGDMA for Hg(II) with the maximum adsorption capacity to Hg(II) of 696.87 mg/g at 30°C in aqueous solution. The increasing Hg(II) concentration would provide the maximum driving force for metal ions to conflict with the mass transfer resistances from the aqueous to adsorbent surface and result in higher probability of collision between the active adsorption sites and Hg(II), thus allowing the active adsorption sites to be completely used, by which a higher adsorption capacity can be realized.

As shown in Table S2 and Figure 8A, the experimental data could be well fitted by the Langmuir isotherm model ($R^2 = 0.9902$) than the Freundlich equation ($R^2 = 0.5427$). The Langmuir model assumes that the adsorption sites are energetically equivalent and identical, and only monolayer adsorption occurs in the process (Weber et al., 1991). The adsorption capacities of Hg(II) onto various adsorbents are listed in Table 2. Compared with other adsorbents, the adsorption capacity of KF@VIM/EGDMA composite for Hg(II) is quite high. Therefore, KF@VIM/EGDMA is a superior adsorbent that has potential application for the removal of Hg(II) from polluted water.

Adsorption Kinetics

The adsorption kinetics of KF@VIM/EGDMA was investigated to determine the adsorption rate which is especially significant for the practical application of an adsorbent. Figure 8B shows the time dependent of Hg(II) adsorption on KF@VIM/EGDMA. The adsorption capacity of the adsorbent for Hg(II) ion shows a rapid increasing with prolonging the contact time, and the adsorption

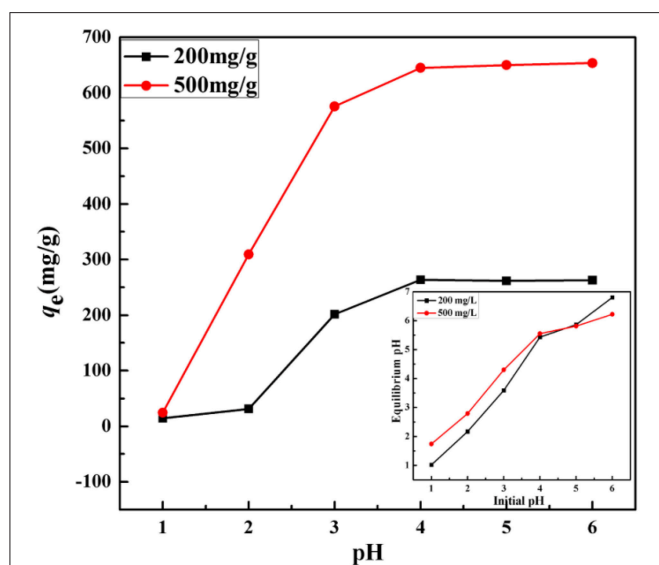


FIGURE 7 | Effect of pH on the adsorption capacity of Hg(II) onto KF@VIM/EGDMA adsorbents. Inset shows the plot of equilibrium pH against initial pH. Adsorption experiments: sample dose: 20 mg/25 mL; t : 120 min; temperature: 30°C.

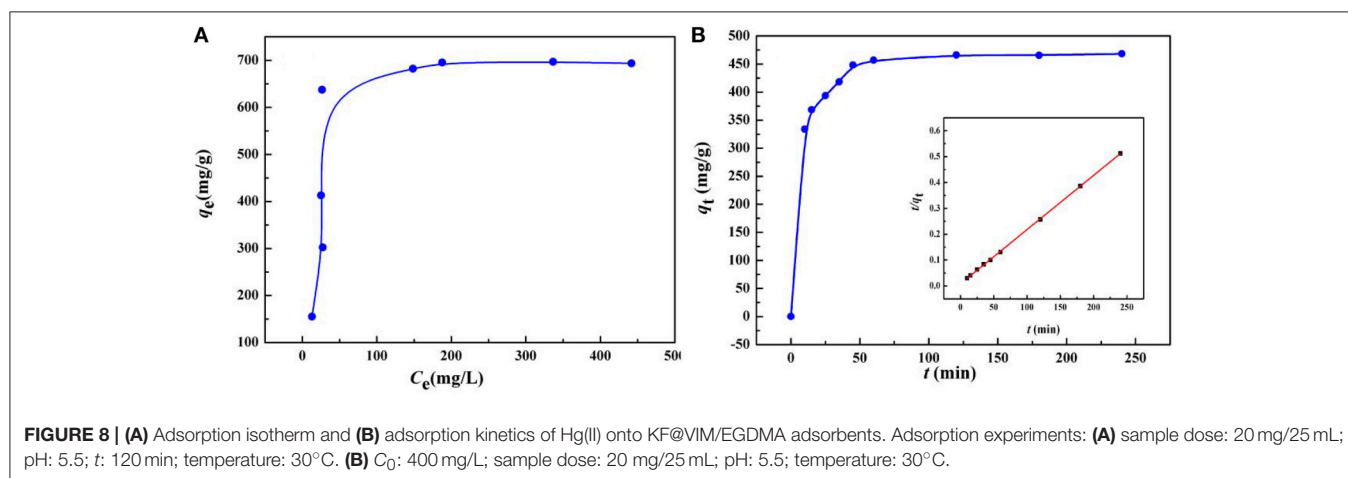


FIGURE 8 | (A) Adsorption isotherm and (B) adsorption kinetics of Hg(II) onto KF@VIM/EGDMA adsorbents. Adsorption experiments: (A) sample dose: 20 mg/25 mL; pH: 5.5; t : 120 min; temperature: 30°C. (B) C_0 : 400 mg/L; sample dose: 20 mg/25 mL; pH: 5.5; temperature: 30°C.

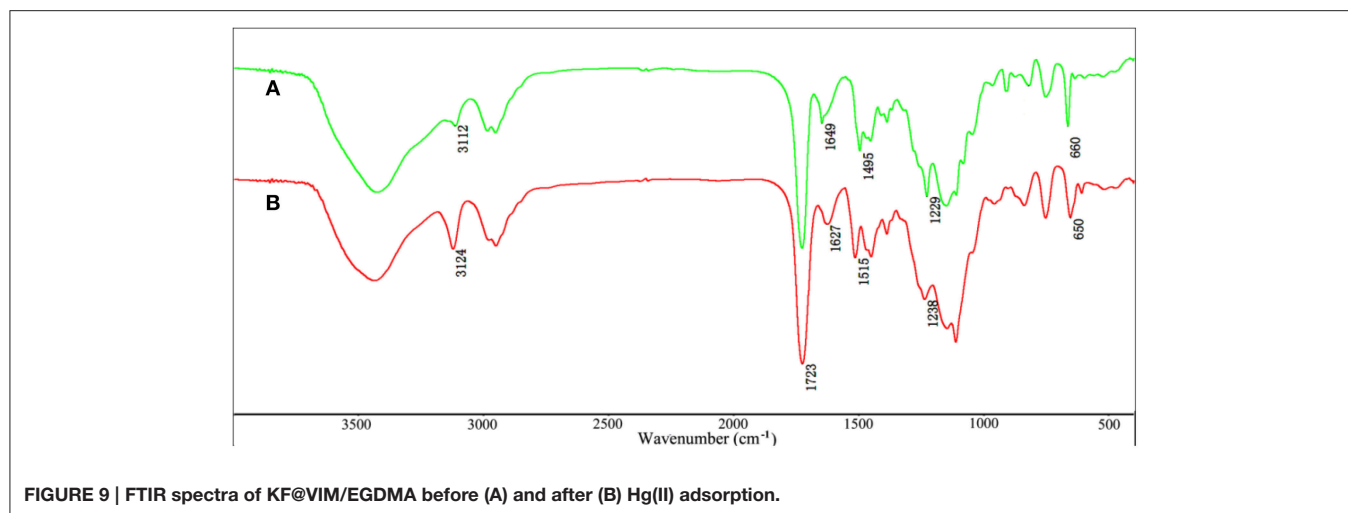


FIGURE 9 | FTIR spectra of KF@VIM/EGDMA before (A) and after (B) Hg(II) adsorption.

TABLE 2 | Maximum adsorption capacity (q_m) of various adsorbents for Hg(II).

| Adsorbents | q_m (mg/g) | References |
|---|--------------|-------------------------|
| Hg-C-TU ^a | 110 | Monier et al., 2014 |
| poly(vinylalcohol)/poly(vinylimidazole) | 120 | Bessbousse et al., 2010 |
| TESM ^b | 139 | Wang et al., 2013b |
| poly(1-vinylimidazole)-grafted Fe ₃ O ₄ @SiO ₂ | 346 | Shan et al., 2015 |
| silica-graft-vinyl imidazole | 356 | Sun et al., 2013 |
| Chitosan-poly(vinylalcohol)/ 10% bentonite | 455 | Wang et al., 2014 |
| Chitosan-poly(vinylalcohol) | 460 | |
| EMCR ^c | 539 | Zhou et al., 2010 |
| polyaniline/humic acid | 671 | Li et al., 2011 |
| KF@VIM/EGDMA | 697 | This study |
| polyaniline/attapulgit composite | 800 | Cui et al., 2012 |
| Polypyrrole-reduced grapheme oxide | 980 | Chandra and Kim, 2011 |

^aHg²⁺ ion-imprinted chelating fibers based on thiourea modified natural cellulosic cotton fibers.

^bThiol functionalized eggshell membrane.

^cEthylenediamine-modified magnetic crosslinking chitosan microspheres.

equilibrium was achieved within 50 min. The experiment date indicate a fast adsorption rate of KF@VIM/EGDMA for Hg(II) removal.

Table S3 indicated that the correlation coefficient values of pseudo-second-order kinetic model ($R^2 = 0.9983$) are much better than that of pseudo-first-order kinetic model ($R^2 = 0.8015$), suggesting that the adsorption process is in line with the pseudo-second-order kinetics model. Otherwise, the close similarities between experimental adsorption capacity (468.39 mg/g) and calculated adsorption capacity value (478.47 mg/g) for Hg(II) once again proved the better fitting of pseudo-second-order kinetic model in comparison to pseudo-first-order kinetic model. All the information presented in Table S3 signified that the pseudo-second-order model is

more appropriate to represent the experimental kinetic data and there is complexation between the Hg(II) and the adsorbent. The chemical adsorption may be the rate-limiting step (Tapaswi et al., 2014).

Adsorption Mechanism

Shifts and changes of FTIR peaks would provide powerful evidence to clarify the adsorption mechanism of Hg(II) onto the functional groups of the as-prepared adsorbent. The chelation between the heavy metal ions and the functional groups will result in the shift of some characteristic absorption bands. The FTIR spectra of KF@VIM/EGDMA before and after Hg(II) adsorption are shown in **Figure 9**. After adsorption, the characteristic absorption bands of VIM were all shifted. For examples, the absorption bands at 3112 cm⁻¹ in the spectrum of KF@VIM/EGDMA was shifted to 3124 cm⁻¹ and the intensity became stronger. The peak at 1495 and 1229 cm⁻¹ were shifted to the high wavenumber at 1515 and 1238 cm⁻¹, respectively. The characteristic peaks at 1649 and 660 cm⁻¹ were shifted to the low wavenumber at 1627 and 650 cm⁻¹ after adsorption. There are no obvious change of the strong band at 1723 cm⁻¹ ascribed to the vibration of C=O after adsorption. All the information listed above indicated that during the adsorption, midazole groups had been participated in the chelation reaction, while carbonyl group was not involved. The X-ray photoelectron spectroscopy (XPS) was also used to investigate the adsorption mechanism of Hg(II) onto the KF@VIM/EGDMA. As shown in **Figure 10**, the appearance of the Hg_{4f} spectrum after the adsorption revealed that the Hg(II) was specifically adsorbed onto KF@VIM/EGDMA. Two photoelectron peaks detected for Hg_{4f7/2} (100.78 eV) and Hg_{4f5/2} (104.88 eV) in **Figure 10C** implied that Hg(II) existed in a divalent state (Wang et al., 2012). Additionally, as shown in the survey spectra in **Figures 10D,E**, after adsorption, the binding energy of the imine (>N-) nitrogen of the imidazole ring at 398.88 eV (Lázaro Martínez et al., 2011) shifted to 399.18 eV, while the amine (-N-C-) nitrogen at 400.78 has no obvious change, demonstrating that the imine (>N-) nitrogen of the imidazole ring mainly chelates with Hg(II) (Sun

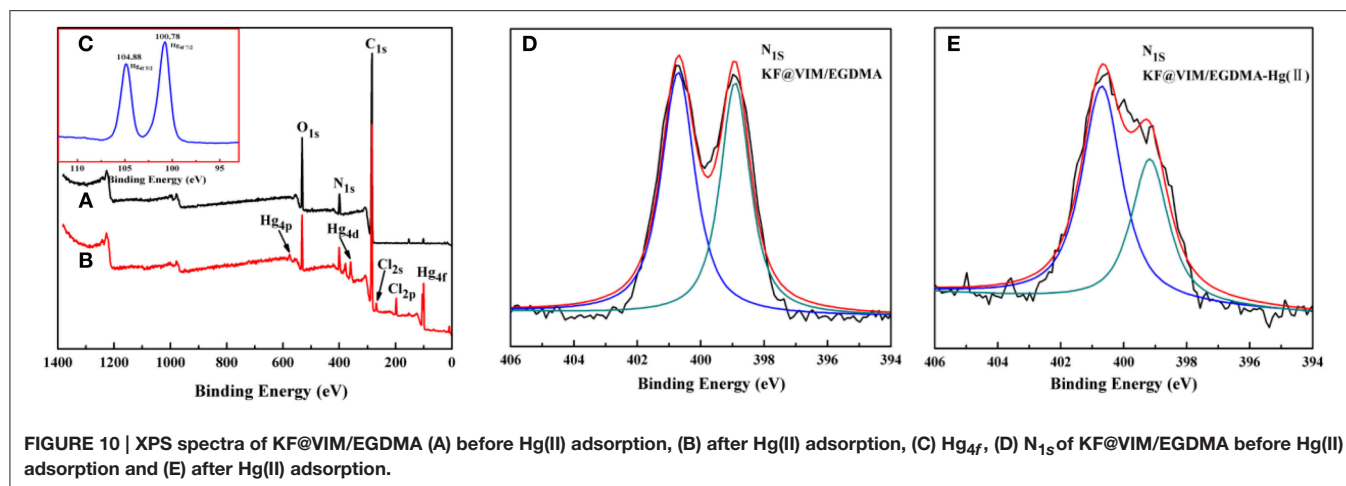


FIGURE 10 | XPS spectra of KF@VIM/EGDMA (A) before Hg(II) adsorption, (B) after Hg(II) adsorption, (C) Hg_{4f}, (D) N_{1s} of KF@VIM/EGDMA before Hg(II) adsorption and (E) after Hg(II) adsorption.

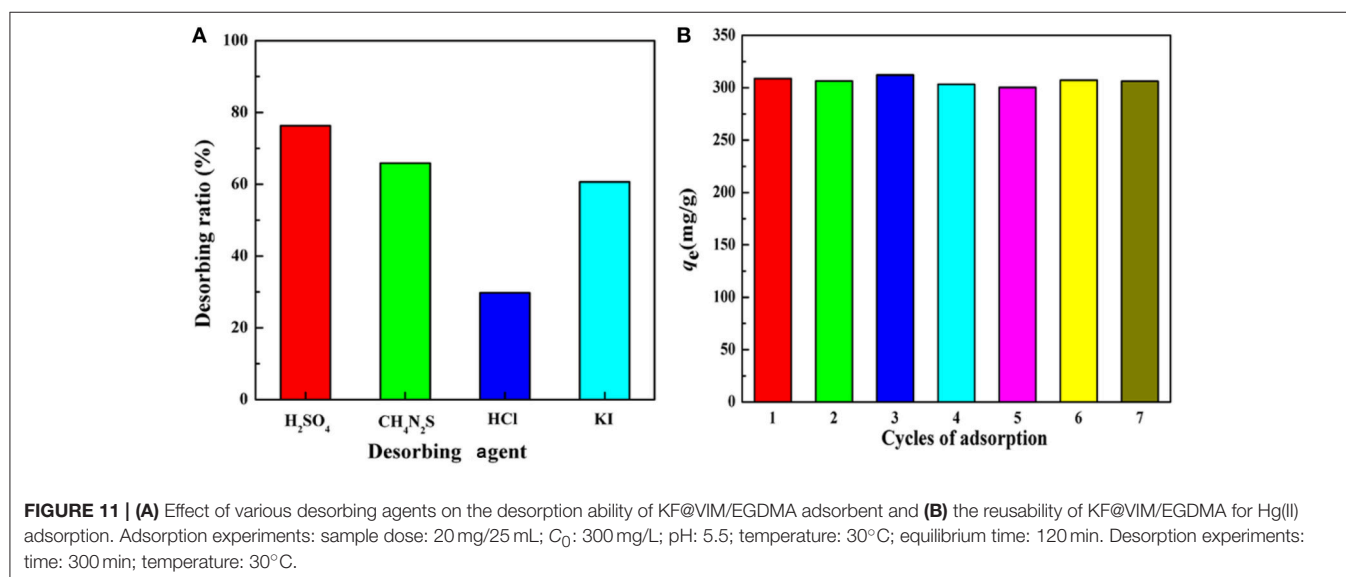


FIGURE 11 | (A) Effect of various desorbing agents on the desorption ability of KF@VIM/EGDMA adsorbent and (B) the reusability of KF@VIM/EGDMA for Hg(II) adsorption. Adsorption experiments: sample dose: 20 mg/25 mL; C₀: 300 mg/L; pH: 5.5; temperature: 30°C; equilibrium time: 120 min. Desorption experiments: time: 300 min; temperature: 30°C.

et al., 2013). The complexation between Hg(II) and nitrogen atoms transferred the electrons from Hg to the imidazole rings, and constructed an electron-rich environment for the nitrogen species, decreasing thus the binding energy of N_{1s} peaks. The probable formation mechanism of mercury-imidazole complex was proposed in **Scheme 1**.

Desorption and Regeneration Performance

The desorption studies and the reusability of the KF@VIM/EGDMA were investigated to evaluate the regeneration and reusabilities of the as-prepared adsorbent.

The species of the desorbing agents would significantly affect the desorption efficiency. Thus, the influences of different desorbing agents with the same concentration on desorption efficiency were investigated. According to the results presented in **Figure 11A**, H₂SO₄ presented the best desorption efficiency among the four desorbing agents. Subsequently, the influences of the concentration of H₂SO₄ on desorption efficiency were performed and the results revealed that the desorption

ratio showed no significant differences by varying H₂SO₄ concentration from 0.1 to 0.9 mol/L. According to the experiment date, 0.5 mol/L H₂SO₄ solution was selected to investigate the regeneration and reusability of the adsorbent. As shown in **Figure 11B**, there appears no significant decrease in the adsorption capacity during the whole adsorption-desorption process, revealing that KF@VIM/EGDMA can be used for multiple cycles, an indication of excellent reusability of the adsorbent for removing Hg(II) from aqueous solution.

CONCLUSIONS

A novel adsorbent KF@VIM/EGDMA composite was designed and developed by a facile and green *in situ* polymerization reaction under mild conditions. The hollow structure and fibrous surface of KF can orientate the polymerization growth, by which a uniform N-containing polymer layer was formed along the KF surface. The as-prepared KF@VIM/EGDMA composite possesses the advantages of excellent adsorption capacity and

selectivity, and fast adsorption kinetics for Hg(II) ions, with the adsorption capacity of as high as 697 mg/g and the adsorption saturation of 45 min. Moreover, the composite based on KF can be separated from the liquid system easily, which is benefit for the recycle of the adsorbent, and the fact of experiment suggested that the as-prepared adsorbent exhibits no obvious retrogress for Hg(II) removal during several adsorption-desorption process. In conclusion, the KF@VIM/EGDMA can be used as an efficiently and economically viable adsorbent for selective adsorption of Hg(II) and the development of the composites coated on natural KF by a facile and green method proposed an effective way to utilize natural resources.

AUTHOR CONTRIBUTIONS

AW: contribute to propose the research idea, design the research programme and revise the research paper. FW: contribute to conducting the research programme and

writing the paper. Y. Zheng: contribute to conducting the research programme and revising the paper. Y. Zhu: contribute to conducting the research programme as an assistant.

ACKNOWLEDGMENTS

This work is supported by the National Natural Science Foundation of China (21377135, 21477135 and 51403221), the Fundamental Research Funds for the Central Universities (lzujbky-2015-127) and Youth Innovation Promotion Association, CAS (2015343).

SUPPLEMENTARY MATERIAL

The Supplementary Material for this article can be found online at: <http://journal.frontiersin.org/article/10.3389/fenvs.2016.00004>

REFERENCES

- Abdullah, M. A., Rahmah, A. U., and Man, Z. (2010). Physicochemical and sorption characteristics of Malaysian *Ceiba pentandra* (L.) Gaertn. as a natural oil sorbent. *J. Hazard. Mater.* 177, 683–691. doi: 10.1016/j.jhazmat.2009.12.085
- Afkhami, A., Saber-Tehrani, M., and Bagheri, H. (2010). Simultaneous removal of heavy-metal ions in wastewater samples using nano-alumina modified with 2,4-dinitrophenylhydrazine. *J. Hazard. Mater.* 181, 836–844. doi: 10.1016/j.jhazmat.2010.05.089
- Ali, N., El-Harabawi, M., Jabal, A. A., and Yin, C. Y. (2011). Characteristics and oil sorption effectiveness of kapok fibre, sugarcane bagasse and rice husks: oil removal suitability matrix. *Environ. Technol.* 33, 481–486. doi: 10.1080/09593330.2011.579185
- Alila, S., and Boufi, S. (2009). Removal of organic pollutants from water by modified cellulose fibres. *Ind. Crops Prod.* 30, 93–104. doi: 10.1016/j.indcrop.2009.02.005
- Bessbousse, H., Rhlalou, T., Verchère, J. F., and Lebrun, L. (2010). Mercury removal from wastewater using a poly(vinylalcohol)/poly(vinylimidazole) complexing membrane. *Chem. Eng. J.* 164, 37–48. doi: 10.1016/j.cej.2010.08.004
- Bourikas, K., Vakros, J., Kordulis, C., and Lycourghiotis, A. (2003). Potentiometric mass titrations: experimental and theoretical establishment of a new technique for determining the point of zero charge (PZC) of metal (hydr)oxides. *J. Phys. Chem. B* 107, 9441–9451. doi: 10.1021/jp035123v
- Chandra, V., and Kim, K. S. (2011). Highly selective adsorption of Hg²⁺ by a polypyrrole-reduced graphene oxide composite. *Chem. Commun.* 47, 3942–3944. doi: 10.1039/c1cc00005e
- Chen, C. Y., Lin, M. S., and Hsu, K. R. (2008). Recovery of Cu(II) and Cd(II) by a chelating resin containing aspartate groups. *J. Hazard. Mater.* 152, 986–993. doi: 10.1016/j.jhazmat.2007.07.074
- Chung, B. Y., Cho, J. Y., Lee, M. H., Wi, S. G., Kim, J. H., Kim, J. S., et al. (2008). Adsorption of heavy metal ions onto chemically oxidized *Ceiba pentandra* (L.) Gaertn. (Kapok) Fibers. *J. Appl. Biol. Chem.* 51, 28–35. doi: 10.3839/jabc.2008.006
- Cui, H., Qian, Y., Li, Q., Zhang, Q., and Zhai, J. (2012). Adsorption of aqueous Hg(II) by a polyaniline/attapulgite composite. *Chem. Eng. J.* 211–212, 216–223. doi: 10.1016/j.cej.2012.09.057
- Duan, C., Zhao, N., Yu, X., Zhang, X., and Xu, J. (2013). Chemically modified kapok fiber for fast adsorption of Pb²⁺, Cd²⁺, Cu²⁺ from aqueous solution. *Cellulose* 20, 849–860. doi: 10.1007/s10570-013-9875-9
- El Ghali, A., Baouab, M. H. V., and Roudesli, M. S. (2012). Aminated cotton fibers loaded with copper(II) ions for enhanced pesticide removal performance from water in a laboratory scale batch. *Ind. Crops Prod.* 39, 139–148. doi: 10.1016/j.indcrop.2012.02.020
- Fan, H., Yu, X., Long, Y., Zhang, X., Xiang, H., Duan, C., et al. (2012). Preparation of kapok-polyacrylonitrile core-shell composite microtube and its application as gold nanoparticles carrier. *Appl. Surf. Sci.* 258, 2876–2882. doi: 10.1016/j.apsusc.2011.10.151
- Huang, X., and Lim, T. T. (2006). Performance and mechanism of a hydrophobic-oleophilic kapok filter for oil/water separation. *Desalination* 190, 295–307. doi: 10.1016/j.desal.2005.09.009
- Idris, S. A., Harvey, S. R., and Gibson, L. T. (2011). Selective extraction of mercury(II) from water samples using mercapto functionalised-MCM-41 and regeneration of the sorbent using microwave digestion. *J. Hazard. Mater.* 193, 171–176. doi: 10.1016/j.jhazmat.2011.07.037
- Ijagbemi, C. O., Baek, M. H., and Kim, D.-S. (2010). Adsorptive performance of un-calcined sodium exchanged and acid modified montmorillonite for Ni²⁺ removal: Equilibrium, kinetics, thermodynamics and regeneration studies. *J. Hazard. Mater.* 174, 746–755. doi: 10.1016/j.jhazmat.2009.09.115
- Kampalananwat, P., and Supaphol, A. P. (2014). The study of competitive adsorption of heavy metal ions from aqueous solution by aminated polyacrylonitrile nanofiber mats. *Energy Procedia* 56, 142–151. doi: 10.1016/j.egypro.2014.07.142
- Kang, P. H., Jeun, J. P., Chung, B. Y., Kim, J. S., and Nho, Y. C. (2007). Preparation and characterization of glycidyl methacrylate (GMA) grafted kapok fiber by using radiation induced-grafting technique. *J. Ind. Eng. Chem.* 13, 956–958.
- Kara, A., Osman, B., Yavuz, H., Beşirli, N., and Denizli, A. (2005). Immobilization of α -amylase on Cu²⁺ chelated poly(ethylene glycol dimethacrylate-n-vinyl imidazole) matrix via adsorption. *React. Funct. Polym.* 62, 61–68. doi: 10.1016/j.reactfunctpolym.2004.08.008
- Keshk, S., Suwinarti, W., and Sameshima, K. (2006). Physicochemical characterization of different treatment sequences on kenaf bast fiber. *Carbohydr. Polym.* 65, 202–206. doi: 10.1016/j.carbpol.2006.01.005
- Kyzas, G. Z., Sifaka, P. I., Lambropoulou, D. A., Lazaridis, N. K., and Bikiaris, D. N. (2014). Poly(itaconic acid)-grafted chitosan adsorbents with different cross-linking for Pb(II) and Cd(II) uptake. *Langmuir* 30, 120–131. doi: 10.1021/la402778x
- Lázaro Martínez, J. M., Rodríguez-Castellón, E., Sánchez, R. M. T., Denaday, L. R., Buldain, G. Y., and Campo Dall'Orto, V. (2011). XPS studies on the Cu(I,II)-polyampholyte heterogeneous catalyst: an insight into its structure and mechanism. *J. Mol. Catal. A: Chem.* 339, 43–51. doi: 10.1016/j.molcata.2011.02.010
- Li, Q., Sun, L., Zhang, Y., Qian, Y., and Zhai, J. (2011). Characteristics of equilibrium, kinetics studies for adsorption of Hg(II) and Cr(VI) by polyaniline/humic acid composite. *Desalination* 266, 188–194. doi: 10.1016/j.desal.2010.08.025

- Lim, T. T., and Huang, X. (2007). Evaluation of kapok (*Ceiba pentandra* (L.) Gaertn.) as a natural hollow hydrophobic-oleophilic fibrous sorbent for oil spill cleanup. *Chemosphere* 66, 955–963. doi: 10.1016/j.chemosphere.2006.05.062
- Liu, X., Zhang, J., Guo, X., Wang, S., and Wu, S. (2012a). Core-shell α -Fe₂O₃@SnO₂/Au hybrid structures and their enhanced gas sensing properties. *RSC Adv.* 2, 1650–1655. doi: 10.1039/C1RA00811K
- Liu, Y., Wang, J., Zheng, Y., and Wang, A. (2012b). Adsorption of methylene blue by kapok fiber treated by sodium chlorite optimized with response surface methodology. *Chem. Eng. J.* 184, 248–255. doi: 10.1016/j.cej.2012.01.049
- Monier, M., Kenawy, I. M., and Hashem, M. A. (2014). Synthesis and characterization of selective thiourea modified Hg(II) ion-imprinted cellulosic cotton fibers. *Carbohydr. Polym.* 106, 49–59. doi: 10.1016/j.carbpol.2014.01.074
- Oo, C. W., Kassim, M. J., and Pizzi, A. (2009). Characterization and performance of *Rhizophora apiculata* mangrove polyflavonoid tannins in the adsorption of copper (II) and lead (II). *Ind. Crops Prod.* 30, 152–161. doi: 10.1016/j.indcrop.2009.03.002
- Prachayawarakorn, J., Chaiwatyothin, S., Mueangta, S., and Hanchana, A. (2013). Effect of jute and kapok fibers on properties of thermoplastic cassava starch composites. *Mater. Design* 47, 309–315. doi: 10.1016/j.matdes.2012.12.012
- Shan, C., Ma, Z., Tong, M., and Ni, J. (2015). Removal of Hg(II) by poly(1-vinylimidazole)-grafted Fe₃O₄@SiO₂ magnetic nanoparticles. *Water Res.* 69, 252–260. doi: 10.1016/j.watres.2014.11.030
- Shen, C., Wang, Y., Xu, J., and Luo, G. (2013). Chitosan supported on porous glass beads as a new green adsorbent for heavy metal recovery. *Chem. Eng. J.* 229, 217–224. doi: 10.1016/j.cej.2013.06.003
- Strelko V. Jr., Malik, D. J., and Streat, M. (2002). Characterisation of the surface of oxidised carbon adsorbents. *Carbon* 40, 95–104. doi: 10.1016/S0008-6223(01)00082-3
- Sun, J., Chen, Z., Ge, M., Xu, L., and Zhai, M. (2013). Selective adsorption of Hg(II) by γ -radiation synthesized silica-graft-vinyl imidazole adsorbent. *J. Hazard. Mater.* 244–245, 94–101. doi: 10.1016/j.jhazmat.2012.11.043
- Talu, M., Demiroğlu, E. U., Yurdakul, Ş., and Badoğlu, S. (2015). FTIR, Raman and NMR spectroscopic and DFT theoretical studies on poly(N-vinylimidazole). *Spectrochim. Acta A* 134, 267–275. doi: 10.1016/j.saa.2014.06.101
- Tapaswi, P. K., Moorthy, M. S., Park, S. S., and Ha, C.-S. (2014). Fast, selective adsorption of Cu²⁺ from aqueous mixed metal ions solution using 1,4,7-triazacyclononane modified SBA-15 silica adsorbent (SBA-TACN). *J. Solid State Chem.* 211, 191–199. doi: 10.1016/j.jssc.2013.12.028
- Uğuzdoğan, E., Denkbaş, E. B., Öztürk, E., Tuncel, S. A., and Kabasakal, O. S. (2009). Preparation and characterization of polyethyleneglycolmethacrylate (PEGMA)-co-vinylimidazole (VI) microspheres to use in heavy metal removal. *J. Hazard. Mater.* 162, 1073–1080. doi: 10.1016/j.jhazmat.2008.05.145
- Wang, J., Zheng, Y., and Wang, A. (2013a). Coated kapok fiber for removal of spilled oil. *Mar. Pollut. Bull.* 69, 91–96. doi: 10.1016/j.marpolbul.2013.01.007
- Wang, S., Wei, M., and Huang, Y. (2013b). Biosorption of multifold toxic heavy metal ions from aqueous water onto food residue eggshell membrane functionalized with ammonium thioglycolate. *J. Agric. Food Chem.* 61, 4988–4996. doi: 10.1021/jf4003939
- Wang, X., Yang, L., Zhang, J., Wang, C., and Li, Q. (2014). Preparation and characterization of chitosan-poly(vinyl alcohol)/bentonite nanocomposites for adsorption of Hg(II) ions. *Chem. Eng. J.* 251, 404–412. doi: 10.1016/j.cej.2014.04.089
- Wang, Y., Yang, H., Pschenitzka, M., Niessner, R., Li, Y., Knopp, D., et al. (2012). Highly sensitive and specific determination of mercury(II) ion in water, food and cosmetic samples with an ELISA based on a novel monoclonal antibody. *Anal. Bioanal. Chem.* 403, 2519–2528. doi: 10.1007/s00216-012-6052-1
- Weber, W. J., McGinley, P. M., and Katz, L. E. (1991). Sorption phenomena in subsurface systems: Concepts, models and effects on contaminant fate and transport. *Water Res.* 25, 499–528. doi: 10.1016/0043-1354(91)90125-A
- Xia, Y., Lu, X., and Zhu, H. (2013). Natural silk fibroin/polyaniline (core/shell) coaxial fiber: Fabrication and application for cell proliferation. *Compos. Sci. Technol.* 77, 37–41. doi: 10.1016/j.compscitech.2013.01.008
- Zheng, Y., Liu, Y., and Wang, A. (2012). Kapok fiber oriented polyaniline for removal of sulfonated dyes. *Ind. Eng. Chem. Res.* 51, 10079–10087. doi: 10.1021/ie300246m
- Zheng, Y., Zhu, Y., and Wang, A. (2014). Kapok fiber structure-oriented polyallylthiourea: Efficient adsorptive reduction for Au(III) for catalytic application. *Polymer* 55, 5211–5217. doi: 10.1016/j.polymer.2014.08.040
- Zhou, L., Liu, Z., Liu, J., and Huang, Q. (2010). Adsorption of Hg(II) from aqueous solution by ethylenediamine-modified magnetic crosslinking chitosan microspheres. *Desalination* 258, 41–47. doi: 10.1016/j.desal.2010.03.051

Conflict of Interest Statement: The authors declare that the research was conducted in the absence of any commercial or financial relationships that could be construed as a potential conflict of interest.

Copyright © 2016 Wang, Zheng, Zhu and Wang. This is an open-access article distributed under the terms of the Creative Commons Attribution License (CC BY). The use, distribution or reproduction in other forums is permitted, provided the original author(s) or licensor are credited and that the original publication in this journal is cited, in accordance with accepted academic practice. No use, distribution or reproduction is permitted which does not comply with these terms.